Synthesis and evaluation of 6-[18F]fluoro-3-(pyridin-3-yl)-1H-indole as potential PET tracer for targeting tryptophan 2, 3-dioxygenase (TDO)

Zheng Qiao, Karine Mardon, Damion Stimson, Mary-anne Migotto, David C. Reutens, Rajiv Bhalla

PII: S0969-8051(19)30507-4

DOI: https://doi.org/10.1016/j.nucmedbio.2019.12.007

Reference: NMB 8108

To appear in: *Nuclear Medicine and Biology*

Received date: 7 October 2019

Revised date: 17 December 2019

Accepted date: 17 December 2019

Please cite this article as: Z. Qiao, K. Mardon, D. Stimson, et al., Synthesis and evaluation of 6-[18F]fluoro-3-(pyridin-3-yl)-1H-indole as potential PET tracer for targeting tryptophan 2, 3-dioxygenase (TDO), *Nuclear Medicine and Biology*(2019), https://doi.org/10.1016/j.nucmedbio.2019.12.007

Synthesis and evaluation of 6-[^{18}F]fluoro-3-(pyridin-3-yl)-1*H*-indole as potential PET tracer for targeting tryptophan 2, 3-dioxygenase (TDO).

Zheng Qiao,[1] Karine Mardon,[1,2] Damion Stimson, Mary-anne Migotto,[1] David C. Reutens[1] and Rajiv Bhalla[1,*]

[1]Centre for Advanced Imaging, The University of Queensland, St Lucia, Brisbane, Queensland 4072, Australia

[2]National Imaging Facility, The University of Queensland, Brisbane, Australia

[*] Corresponding author

E-mail: r.bhalla@uq.edu.au

Abstract

Introduction: The increase in expression of tryptophan 2, 3-dioxygenases (TDO) and indoleamine 2,3-dioxygenase (IDO) have been reported as potential tumor biomarkers. TDO and IDO are enzymes that catalyze the first and rate-limiting step of the kynurenine pathway. Positron emitting tomography (PET) tracers investigating the kynurenine pathway may allow for the detection of different disease pathologies *in vivo* including cancer. However, current PET tracers being developed for TDO and IDO have suffered from either multi-step low yielding syntheses or de-fluorination of the tracer *in vivo*.

Results: TDO inhibitors based on 6-fluoroindole with C3 substituents are a class of small molecules that have been shown to bind to TDO effectively, restore tryptophan concentration and decrease the production of immunosuppressive metabolites. The compound 6-fluoro-3-(pyridine-3-yl)-1*H*-indole has been reported to have high *in vitro* affinity for TDO. Herein we report the fully automated radiosynthesis of 6-[^{18}F]fluoro-3-(pyridine-3-yl)-1*H*-indole [^{18}F]**4** using a copper-mediated nucleophilic ^{18}F-fluorination resulting in a non-corrected yield of 5 to 6 % of the tracer with a radiochemical purity of > 99% after 4 hours. Small animal dynamic PET/CT imaging of [^{18}F]**4** intravenously injected into normal C57BL/6 mice revealed rapid accumulation in heart and brain, reaching maximum occupancy in heart (10.9% ID/g) and brain (8.1% ID/g) at 1.75 min and 2.25 min, respectively. Furthermore, these *in vivo* studies revealed no de-fluorination of the tracer, as evidence by the absence of [^{18}F]fluoride accumulation in bone.

Conclusion: *In vitro* studies demonstrate that **4** has good affinity for hTDO and the radiolabeled analogue [^{18}F]**4** can be synthesized with suitable radiochemical yields. [^{18}F]**4** demonstrates good uptake in the brain and the radiolabeled compound shows no de-fluorination *in vivo* in C57BL/6 mice.

Keywords: TDO inhibitor, 6-fluoroindole, PET, biodistribution, fluorine-18

1. Introduction

Tryptophan is an essential amino acid which is metabolized predominantly via the kynurenine pathway by the enzymes tryptophan 2,3-dioxygenase (TDO) and indoleamine 2,3-dioxygenase (IDO). These enzymes are overexpressed in a wide variety of tumors especially in glioblastoma.[1] TDO and IDO catalyze the first and rate-limiting step of the kynurenine pathway in which the oxidative indole ring cleavage reaction of tryptophan to *N*-formyl-kynurenine is achieved by employing molecular oxygen or reactive oxygen species across the C2-C3 bond (**Figure 1**).[2] Inhibition of tryptophan metabolism using TDO or IDO inhibitors and the subsequent restoration of tryptophan concentration by could prove to be a beneficial strategy in the context of disease progression in cancer.[3, 4]

Monitoring the upregulation of IDO and TDO using PET tracers has been the focus of several research groups for tumor detection. The majority of these PET tracers are radiolabeled derivatives of tryptophan including α-[^{11}C]methyl-*L*-tryptophan ([^{11}C]AMT)[5], 1-*N*-[^{11}C]methyl-*L/D*-tryptophan (*L/D*-[^{11}C]1MTrp)[6], 1-*N*-[^{18}F]fluoroethyl-*L/D*-tryptophan (1-*L/D*-*N*-[^{18}F]FETrp)[7], 4, 5, 6-[^{18}F]fluorotryptophan (4, 5, 6-[^{18}F]FTrp)[8, 9] (**Figure 2**). However only [^{11}C]AMT has been widely investigated in clinical studies imaging IDO-upregulated tumors, especially for patients with glioblastoma.[10, 11] However, the wider utility of [^{11}C]AMT has been limited because of complex radiosynthesis of this radiotracer and short half-life of carbon-11 (20 minutes).[12, 13] The other tracers have either (i) demonstrated poor uptake of the tracers in the brain or (ii) involved multistep radiosyntheses or (iii) shown defluorination of the tracer *in vivo*.[6-9] These results indicate that the need for the development of PET tracers (ideally fluorine-18 tracers) which show good affinity to IDO / TDO and are easy to synthesize and show minimal defluorination *in vivo*.

The 6-fluoroindole moiety has been demonstrated to be a potential useful building block for the design and synthesis of IDO and TDO inhibitors. Whilst 6-fluoro-tryptophan exhibits high *in vitro* affinity to TDO,[14] recent studies of the fluorine-18 labeled analogue have demonstrated de-fluorination of the radiotracer *in vivo*. Indole derivatives with substituents at the C3 position exhibit

pico- to nanomolar inhibitory actions against a wide range of biological targets and processes.[15, 16] Consequently C3 substituents of 6-fluoroindole have been synthesized and evaluated in terms of their solubility and *in vitro* activity to TDO.

In this present study, we report the synthesis and initial pre-clinical evaluation of a radiolabeled TDO inhibitor. This radiolabeled agent 6-[^{18}F]]fluoro-3-(pyridine-3-yl)-1*H*-indole [^{18}F]**4** contains a 6-fluoroindole moiety with substituents on the C3 position. The non-radioactive analogue 6-fluoro-3-(pyridine-3-yl)-1*H*-indole has an IC_{50} of 850 nM in an enzymatic assay.[16]

2. Experimental

2.1. Materials and instruments

All chemicals and solvents were purchased from Sigma-Aldrich and used as received without further purification. Thin-layer chromatography (TLC) was performed on pre-coated silica gel 60 F254 M (Merck, Darmstadt, Germany) with UV detection at 254 nm . Milli-Q water was used throughout the experiments. Human TDO with a concentration of 2.87 mg/mL was obtained from BPS Bioscience. Sep-Pak® Accel Plus QMA Carbonate Light Cartridge (46 mg sorbent/cartridge, 40 μm particle size, p/n 186004540, Waters) was purchased and used as received. Sep-Pak® C18 Plus Light Cartridge (130 mg sorbent/cartridge, p/n WAT023501) was also purchased from Waters® and conditioned before use with 10 mL of ethanol, then 10 mL of water and finally 20 mL of air.

^{1}H and ^{13}C NMR spectrum were recorded on Bruker-500 or 900 Hz spectrometers at ambient temperature, the chemical shifts (δ) were reported as ppm in $CDCl_3$ or DMSO-d_6. Mass spectra (MS) data were acquired on Bruker Autoflex Speed MALDI-TOF MS in positive mode, using α-cyano-4-hydroxycinnamic acid (CHCA) as the matrix (matrix-free for radiolabelling precursor **8**). The UV-vis adsorption at specific wavelength were recorded on Thermal Scientific Nanodrop 2000/2000c. No-carried-added [^{18}F]fluoride was generated using an 18 MeV cyclotron (Cyclone "Twin" 18/18 MeV, IBA). The fully automated radiosynthesis was carried out on commercially

available Synthra RN_{plus} (Synthra, GmbH) module. Analytical HPLC studies were performed using Shimadzu and Agilent systems equipped with UV and radiation detection.

2.2. Chemistry

*2.2.1. Synthesis of tert-butyl 6-fluoro-3-iodo-1H-indole carboxylate (**1**)*

The Boc protection to form compound **1** was carried out using a procedure analogous to that used for the synthesis of *tert*-butyl 3-iodo-1H-indole-1-carboxylate.[17] A solution of iodine (13.2 mmol, 3.35 g) in 20 mL of DMF was dropped to the solution of 6-fluoroindole (12 mmol, 1.62 g) and KOH (30 mmol, 1.68 g) in 20 mL of DMF at room temperature. The mixture was stirred overnight, followed by adding to 300 mL of cold H_2O containing sodium metabisulphite (6 g, 2%) and ammonia (3 g, 1%). The mixture was extracted with Et_2O and dried over Na_2SO_4, filtered and concentrated. The obtained concentrate was suspended in dichloromethane (100 mL). DMAP (2.4 mmol, 0.29 g), triethylamine (2.4 mmol, 0.24 g) and $(Boc)_2O$ (14.4 mmol, 3.14 g) were added to the reaction mixture. The reaction was allowed to stir at room temperature overnight. Saturated NH_4Cl and dichloromethane were added to the reaction mixture and the organic layer extracted. The combined organic layers were dried over Na_2SO_4, filtered and concentrated. Chromatographic purification (40% EtOAc in hexane) afforded desired compound as a brown solid (1.30 g, 79% yield, Rf = 0.88). ^{1}H NMR (500 MHz, $CDCl_3$): δ 7.87 (d, J = 9.8 Hz, 1H), 7.69 (s, 1H), 7.32 (dd, J = 8.7, 5.3 Hz, 1H), 7.06 (td, J = 8.9, 2.4 Hz, 1H), 1.66 (s, 9H). ^{13}C NMR (125 MHz, $CDCl_3$) δ 161.7, 148.6, 130.6, 128.6, 122.6, 122.5, 111.9, 111.7, 102.6, 102.4, 84.9, 64.9, 28.3.

*2.2.2. Synthesis of 3-(4,4,5,5,-tetramethyl-1,3,2-dioxaborolan-2-yl)pyridine (**2**)*

The title compound was prepared as described by Andersen *et al.*[18] A solution of 3-bromopyridine (10 mmol, 1.58 g) in 5 mL of Et_2O was slowly added to a 2.5 M hexane solution of n-BuLi (12 mmol, 4.8 mL) in 50 mL of Et_2O at -78°C. The reaction mixture was stirred for 30 min and then trimethoxyborane (12 mmol, 1.34 mL) was slowly added to the reaction mixture at -78°C. The reaction mixture was warmed to room temperature and left under stirring for 24 h. Pinacol (10.5

mmol, 1.24 g) was added to the solution and stirred for 1 h. Acetic acid (2.2 mmol, 1.26 mL) was added to the reaction mixture and left stirring for a further 6 h. The mixture was then concentrated and the extracted with dichloromethane. The crude product was concentrated to afford an off-white solid. The resultant solid was washed with CH_3CN to afford desired compound (1.65 g, 80% yield). ^{1}H NMR (500 MHz, $CDCl_3$): δ 8.95 (s, 1H), 8.67 (dd, J = 4.9, 1.9 Hz 1H), 8.05 (dt, J = 7.5, 1.7 Hz 1H), 7.30 – 7.27 (m, 1H), 1.36 (s, 12H). ^{13}C NMR (125 MHz, $CDCl_3$): δ 155.6, 152.1, 142.3, 123.2, 84.3, 25.0.

*2.2.3. Synthesis of tert-butyl 6-fluoro-3-(4,4,5,5-tetramethyl-1,3,2-dioxaborolan-2-yl)-1H-indole-1 carboxylate (**3**)*

The incorporation of the boronate ester was performed using two different synthetic routes using chemical methodologies as described by Jia *et al*.[19] (synthetic route 1) and Sigala *et al*[20] (synthetic route 2) with minor modification. *Synthetic route* 1: **1** (3 mmol, 1.08 g), bis(pinacolato)diboron (6 mmol, 4.52 g), KOAc (9 mmol, 0.88 g) and Pd(dppf)Cl_2 (0.09 mmol, 0.07 g) were mixed under nitrogen. 30 mL of 1, 4-dioxane was added to the flask under nitrogen. The resultant mixture was heated at 80°C overnight. The solvent was removed after a crude purification by silica gel column to remove the catalyst. Chromatographic purification (10% Et_2O in hexane) afforded desired compound as white solid (0.21 g, 19.5% yield, Rf = 0.37). ^{1}H NMR (500 MHZ, CDCl3): δ 7.96 (s, ^{1}H), 7.88 (dd, J = 8.6, 5.7 Hz, 2H), 7.00 (td, J = 9.0, 2.4 Hz, 1H), 1.36 (s, 12H). ^{13}C NMR (125 MHz, $CDCl_3$): δ 159.7, 148.1, 134.3, 128.5, 122.2, 110.1, 109.9, 101.3, 101.1, 83.2 (2C), 82.6, 27.1 (3C), 23.8 (4C).

Synthetic route 2: **1** (3 mmol, 1.08 g) and Pd(dppf)Cl_2 (0.09 mmol, 0.07 g) were mixed under nitrogen. Degassed toluene (15 mL) was added, and the mixture was degassed for another 5 min with N_2. Et_3N (11.4 mmol, 1.15 g) and pinacolborane (4.57 mmol, 0.58 g) were successively added to the reaction mixture. The mixture was heated at 80°C for 3 h. The solvent was removed to leave the crude compound which was then purified by column chromatography (10% Et_2O in hexane) to give the desired compound as a white solid (0.87 g, 81% yield, Rf = 0.37). ^{1}H NMR (500 MHz,

$CDCl_3$): δ 7.96 (s, 1H), 7.88 (dd, J = 8.6, 5.7 Hz, 2H), 7.00 (td, J = 9.0, 2.4 Hz, 1H), 1.36 (s, 12H). ^{13}C NMR (125 MHZ, $CDCl_3$): δ 159.7, 148.1, 134.3, 128.5, 122.2, 110.1, 109.9, 101.3, 101.1, 83.2 (2C), 82.6, 27.1 (3C), 23.8 (4C).

*2.2.4. Synthesis of 6-fluoro-3-(pyridin-3-yl)-1H-indole (**4**)*

6-fluoro-3-(pyridin-3-yl)-1H-indole was prepared by two different Pd-catalyzed cross-coupling methodologies as described by Song *et al*[21] (synthetic route 1) and Okada *et al*[22] (synthetic route 2). *Synthetic route 1*: to a suspension of **3** (0.75 mmol, 0.27 g) in degassed co-solvent composed of 1, 4-dioxane (15 mL) and H_2O (5 mL), 3-bromopyridine (0.75 mmol, 0.12 g) and K_3PO_4 (1.5 mmol, 0.32 g) were added under nitrogen. And then $Pd(dppf)Cl_2$ (0.08 mmol, 0.06 g) was added under nitrogen. The reaction was heated at 100°C for 18 h. The reaction mixture was then extracted with EtOAc, dried over Na_2SO_4, filtered and concentrated. Chromatographic purification (50% EtOAc in hexane) afforded desired compound as a brown solid (0.02 g, 12.5% yield, Rf = 0.17). ^1H NMR (500 MHz, $CDCl_3$): δ 8.89 (d, 1H), 8.60 (s, 1H), 8.53 (dd, J = 4.9, 1.6 Hz 1H), 7.99 (dt, J = 7.9, 1.9 Hz 1H), 7.77 (dd, J = 8.8, 5.2 Hz 1H), 7.44 – 7.39 (m, 2H), 7.15 (dd, J = 9.3, 2.3 Hz 1H), 6.99 (td, J = 9.1, 2.3 Hz 1H). ^{13}C NMR (125 MHz, $CDCl_3$): δ 160.2, 147.1, 145.9, 136.7, 135.3, 131.7, 124.0, 122.7, 121.9, 120.1, 114.3, 109.7, 98.0. MS (MALDI-TOF, $[M + H]^+$) calcd for $C_{13}H_{10}FN_2$ 213.23, found 213.10.

Synthetic route 2: **1** (3 mmol, 1.08 g), 3-(4, 4, 5, 5,-tetramethyl-1, 3, 2-dioxaborolan-2-yl)pyridine (2.5 mmol, 0.51 g), K_2CO_3 (12.6 mmol, 1.74 g), and $Pd(dppf)Cl_2$ (0.09 mmol, 0.07 g) were mixed under nitrogen. 20 mL of degassed DMSO was added to the flask under nitrogen. The reaction mixture was heated at 90°C for 3 h and subsequently H_2O was added to quench the reaction. The reaction mixture was extracted with EtOAc, dried over Na_2SO_4, filtered and concentrated. The residue was purified by silica gel column chromatography (50% EtOAc in hexane) to afford the product as a brown solid (0.19 g, 30% yield, Rf = 0.17). ^1H NMR (500 MHz, $CDCl_3$): δ 8.89 (d, 1H), 8.60 (s, ^1H), 8.53 (dd, J = 4.9, 1.6 Hz 1H), 7.99 (dt, J = 7.9, 1.9 Hz 1H), 7.77 (dd, J = 8.8, 5.2 Hz 1H), 7.44 – 7.39 (m, 2H), 7.15 (dd, J = 9.3, 2.3 Hz 1H), 6.99 (td, J = 9.1, 2.3 Hz 1H). ^{13}C NMR

(125 MHz, $CDCl_3$): δ 160.2, 147.1, 145.9, 136.7, 135.3, 131.7, 124.0, 122.7, 121.9, 120.1, 114.3, 109.7, 98.0. MS (MALDI-TOF, $[M + H]^+$) calcd for $C_{13}H_{10}FN_2$ 213.23, found 213.10.

*2.2.5. Synthesis of tert-butyl 6-bromo-3-iodo-1H-indole carboxylate (**5**)*

The boc protection to form compound **5** was carried out using an analogous procedure for that used in the synthesis of tert-butyl 3-iodo-1H-indole-1-carboxylate as described by Witulski *et al.*[17] A solution of iodine (4.4 mmol, 1.12 g) in DMF (30 mL) was added to a solution of 6-bromoindole (4 mmol, 0.78 g) and KOH (10 mmol, 0.56 g) in DMF (30 mL) at room temperature. The mixture was stirred overnight, followed by addition to 300 mL of cold H_2O containing sodium metabisulphite (6 g, 2%) and ammonia (3 g, 1%). The mixture was extracted by Et_2O and dried over Na_2SO_4, filtered and concentrated. This was suspended in dichloromenthane (100 mL) and then DMAP (0.8 mmol, 0.09 g), Et_3N (0.8 mmol, 0.08 g) and $(Boc)_2O$ (4.8 mmol, 1.05 g) were added. The reaction was allowed to stir at room temperature overnight. Saturated NH_4Cl and dichloromethane were added to the reaction mixture and the organic layer extracted. The combined organic layers were dried over Na_2SO_4, filtered and concentrated. Chromatographic purification (40% EtOAc in hexane) afforded desired compound as a brown solid (1.18 g, 70% yield, Rf = 0.88). ^{1}H NMR (500 MH_Z, $CDCl_3$): δ 8.35 (s, 1H), 7.67 (s, 1H), 7.42 (dd, *J* = 8.4, 1.7 Hz 1H), 7.25 (d, 1H), 1.66 (s, 9H). ^{13}C NMR (125 MH_Z, $CDCl_3$) δ 147.1, 130.0, 129.5, 125.6, 121.6, 118.3, 117.2, 83.9, 63.8, 28.7, 27.0 (3C).

*2.2.6. Synthesis of 6-bromo-3-(pyridin-3-yl)-1H-indole (**6**)*

Compound 6 was prepared using Pd-catalyzed cross coupling methodologies as described by Okada *et al.*[22] **5** (2.5 mmol, 1.05 g), 3-(4,4,5,5,-tetramethyl-1,3,2-dioxaborolan-2-yl)pyridine (2.1 mmol, 0.43 g), and K_2CO_3 (10.4 mmol, 1.44 g) were mixed under nitrogen. 30 mL of degassed DMSO was added to the flask under N_2. The reaction mixture was heated at 90°for 3 h. H_2O was added to quench the reaction. The reaction was extracted with EtOAc, dried over Na_2SO_4, filtered and concentrated. The residue was purified by silica gel column chromatography (50% acetone in hexane) to afford product as a brown solid (0.15 g, 22% yield, R_f = 0.56). ^{1}H NMR (500 MH_Z, DMSO-d_6): δ 11.63 (s, 1H), 8.89 (dd, *J* = 2.4, 0.9 Hz 1H), 8.43 (dd, *J* = 4.7, 1.6 Hz 1H), 8.05 (ddd,

J = 7.9, 2.4, 1.6 Hz 1H), 7.85 (s, 1H), 7.81 (d, *J* = 8.5 Hz 1H), 7.64 (d, *J* = 1.8 Hz 1H), 7.43 (ddd, *J* = 7.9, 4.8, 0.9 Hz 1H), 7.22 (dd, *J* = 8.5 Hz 1H). ^{13}C NMR (125 MH_Z, DMSO-d_6): δ 147.9, 147.2, 138.4, 134.1, 131.6, 125.8, 124.5, 124.4, 123.4, 121.3, 115.2, 114.9, 113.1. MS (MALDI-TOF, $[M]^+$) calcd for $C_{13}H_9BrN_2$ 273.13, found 273.01.

*2.2.7. Synthesis of 3-(pyridin-3-yl)-6-(4,4,5,5-tetramethyl-1,3,2-dioxaborolan-2-yl)-1H-indole (**7**)*

The incorporation of the boronate ester was carried out using analogous methods to those described by Taylor *et al.*[23] **6** (0.26 mmol, 0.07 g), bis(pinacolato)diboron (0.51 mmol, 0.13 g), KOAc (0.77 mmol, 0.075 g), and Pd(dppf)Cl_2 (0.026 mmol, 0.02 g) were mixed under N_2. 3 mL of degassed toluene was added and the reaction mixture was heated at 90°C for 24 h. H_2O was added to quench the reaction. The reaction mixture was extracted with EtOAc, dried over Na_2SO_4, filtered and concentrated. The catalyst was removed by silica gel column chromatography (50% acetone in hexane) to afford crude product and used for the next step.

*2.2.8. Synthesis of tert-butyl 3-(pyridin-3-yl)-6-(4,4,5,5-tetramethyl-1,3,2-dioxaborolan-2-yl)-1H-indole-1-carboxylate (**8**)*

Boc protection was carried out using a process analogous to that described by Tasch *et al.*[24] **7** (0.09 mmol, 0.03 g) was suspended in dichoromethane (3 mL), followed by the addition of DMAP (0.02 mmol, 0.002 g), Et_3N (0.02 mmol, 0.002 g) and $(Boc)_2O$ (0.11 mmol, 0.02 g). The reaction mixture was stirred at room temperature for 1 h. The solvent was removed by rotary evaporator to leave the crude compound which was purified by HPLC to give the desired compound as a white solid (0.037 g, 0.09 mmol, 98% yield). Eclipse XDB-C18 Semi-Prep 5µm, 9.4 × 250mm, p/n 990967-202). Mobile phase: 70% MeCN in water with a constant flow rate of 4 mL/min. ^{1}H NMR (500 MH_Z, $CDCl_3$): δ 9.02 (s, 1H), 8.80 (s, 1H), 8.66 (m, 1H), 8.57 (d, 1H), 7.98 (s, 1H), 7.91 (s, 1H), 7.81 (dd, *J* = 7.9, 1.0 Hz, 1H), 7.75 (m, 1H), 1.36 (s, 12H), 1.66 (s, 9H). ^{13}C NMR (225 MHz, DMSO-d_6): δ 148.7, 148.3, 148.3, 135.1, 134.9, 130.2, 128.9, 128.8, 125.3, 123.4, 121.4, 119.1, 117. 8, 84.3, 83.7 (2C), 54. 9, 27.6 (3C), 24.7 (4C). MS (MALDI-TOF, $[M + H]^+$) calcd for $C_{24}H_{30}BN_2O_4$ 421.32, found 421.25.

*2.3. Final optimized radiosynthesis of [^{18}F]**4***

[^{18}F]Fluoride in oxygen-18 enriched water (98%) was transferred using helium pressure to the hot-cell where it was measured in a dose calibrator and then transferred into the "V-vial" of the Synthra RN_{Plus} synthesis module. The aqueous [^{18}F]F^- was transferred under vacuum *via* valve V1 to the QMA cartridge with the enriched water directed to a $H_2{}^{18}O$ recovery vial *via* V13. The [^{18}F]F^- was eluted from the cartridge via V13, and V14 and collected in the glassy carbon reaction vessel using a 1 mL solution containing 4 mg Kryptofix® (10.6 µmol) and K_2CO_3 (0.69 mg, 5 µmol) in 1 mL (50:50 water : MeCN). Drying of the fluoride was performed using helium flow (V18) with vacuum applied (V19, V22) at a temperature of 68°C for 5 minutes, then at 95°C for a further 10 minutes. Helium flow ceases and the reaction vessel was cooled to 30°C before the vacuum was stopped. A solution of the precursor **8** (7 µmol) and $[Cu(py)_4](OTf)_2$ (9 µmol) in 1 mL of DMA was transferred from vial A3 into the reaction vessel, followed by addition of 1 mL of air from the syringe. Radiolabeling was carried out at 120°C for 10 minutes, followed by thermal deprotection by heating at 150°C for 5 minutes. The reaction vessel was then cooled to 30°C and water (1mL) was added from vial A4. The diluted crude reaction mixture was drawn-up into the syringe unit using position 3 of the syringe valve. The syringe unit was used to load the 5mL volume HPLC loop with the diluted crude reaction mixture via position 2 of the syringe valve and injected onto the HPLC column using V26. Semi-preparative HPLC purification was carried out using isocratic conditions with an Eclipse XDB-C18 Semi-Prep 5µm (9.4 mm × 250 mm; p/n 990967-202). Mobile phase: 40% MeCN / 60% 0.1 M NH_4OAc (with 10 mg / mL of sodium ascorbate in the mobile phase) with a flow rate of 4 mL/min.

The purified product was cut to a collection vial containing 40 mL of water (containing 10 mg / mL of sodium ascorbate) via V27 and stirred. Helium pressure was applied to the vial to transfer the contents through a manually preconditioned (10 mL EtOH, 10 mL water then 20 mL air) C18 cartridge (Sep-Pak® C18 light Cartridge, Waters, p/n WAT023501) to waste via V35 and V36.

The loaded C18 Sep-Pak cartridge was then washed with 10mL of water from vial C3 directly to waste. [^{18}F]**4** was eluted from the C18 cartridge with 1 mL ethanol from C2 to the vented product collection vial containing 9 mL of 0.9% saline (containing 100 mg of sodium ascorbate). The total synthesis time (which has not been optimized) from ^{18}F delivery to reformulated product collection was under 70 minutes.

2.4. Manual labeling experiments

Methods and equipment used to test the labelling at low activity have recently been described by Stimson et al.[25]

*2.5. Quality control (QC) of [^{18}F]**4***

[^{18}F]4 was injected on analytical HPLC connected with a gamma-detector for the determination of radiochemical yield (RCY), and radiochemical stability and purity. Injection with reference compound **4** was conducted to determine the identity of [^{18}F]**4**. The radiochemical stability was checked up to 4 hours after the end of synthesis (EOS) at room temperature.

All analytical HPLC methods in this paper have used an Eclipse Plus C18 column, 5 µm (46 × 150 mm, Agilent, Part NO. 959993-902) using 0.1M ammonium acetate as solvent A and MeCN as solvent B at a flow rate of 1 mL/ min. The method for the analysis for the HPLC traces in **Figure 3** (HPLC Method 1) was 0 to 1 min (30% B), 1 to 25 min (30 to 95% B), 25 to 30 min (95% B), 30 to 31 min (95 to 30% B), 31 to 33 min (30% B). The method for the final QC analysis for the HPLC traces (HPLC Method 2) in **Figure 6** was 0 to 20 min (40% B), 20 to 21 min (40 to 90% B), 21 to 26 min (90% B), 26 to 27 min (90 to 30% B), 27 to 30 min (40% B).

*2.6. Determination of lipophilicity (logD) of **4***

In order to measure the distribution coefficient, 2 mg of **4** was simply dispersed into 2 mL of n-octanol / 0.2 M sodium phosphate buffer system pH 7.5 (1:1, v:v). The vial was strongly vortexed for 5 min and centrifuged at 13000 rpm for another 5 min. An aliquot of each layer (100 µL) was

taken off and measure under UV-vis. LogD was calculated as the decimal logarithm of the ratio between the UV-vis absorption in the n-octanol phase and the buffer phase.

2.7. In vitro enzymatic essay

2.7.1. Establishment of kynurenine standard curve

The kynurenine standard was established according to the literature with minor modification.[26] The standard assay mixture (200 μL) contained 76 μL of 1 M potassium phosphate buffer (pH = 6.5), 20 μL of 0.4 M sodium ascorbate, 4 μL of 1 mM methylene blue, 40 μL of 1 mg/mL catalase, and different amount of 1 mM kynurenine (25 to 45 μL). 40 μL of 30% trichloroacetic acid was added to each vial. After centrifugation at 13000 rmp for 15 min, aliquots of 125 μL of supernatant was mixed with 125 μL of 2% p-dimethylaminobenzaldehyde and measured under UV-vis of Nanodrop 2000/2000c at 480 nm.

2.7.2. In vitro enzymatic essay of TDO

The in vitro enzymatic essay of TDO was performed according to the literature with minor modification.[27] A standard reaction vial (200 μL) contained 86 μL of 1 M potassium phosphate buffer (pH = 6.5), 20 μL of 0.4 M sodium ascorbate, 4 μL of 1 mM methylene blue, 40 μL of 1 mg/mL catalase, 20 μL of different concentrations of L-tryptophan (0.4, 0.8, 1.6, 3.2, and 6.4 mM), 10 μL of 1 mM 6-fluoro-3-(pyridine-3-yl)-1*H*-indole and 20 μL of 0.5 μM of TDO. Each vial was incubated at 37 ^{o}C for 60 min and then 40 μL of 30% trichloroacetic acid was added, followed by further incubation at 65 ^{o}C for 20 min. After centrifugation at 13000 rmp for 15 min, aliquots of 125 μL of supernatant was mixed with 125 μL of 2% *p*-dimethylaminobenzaldehyde and measured under UV-vis of Nanodrop 2000/2000c at 480 nm.

2.8. In vivo PET/CT imaging studies

All animal experiments were approved by the University of Queensland Ethics committee and carried out at the Centre for Advanced Imaging, UQ. PET/CT images were acquired using an Inveon multimodality PET/CT scanner (Siemens). On the experimental days, 6 healthy female

C57BL/6 mice were anaesthetized with 2-3% isoflurane (IsoFlo, Abbott Laboratories) in oxygen at a flow of 2 L/min. A catheter was inserted into the lateral tail vein before the animal was placed in the scanner. Mice were maintained under 1 – 2% isoflurane in air-oxygen mixture at a flow rate of 2L/min for the duration of the imaging session. Physiological monitoring (respiratory using a sensor probe) was achieved throughout all experiments using an animal monitoring system (BioVet system, m2m Imaging, Australia). A single intravenous injection of the tracer was performed with a total injected volume not greater than 200 μL, containing not greater than 15 MBq of tracer in a solution of 10% EtOH in saline. A 60 min dynamic PET scan was started simultaneously with the tracer injection and was followed by a 15 min CT attenuation scan.

The CT images of the mice were acquired through an X-ray source with the voltage set to 80 kV and the current set to 500 μA. The scans were performed using 360^{o} rotation with 120 rotation steps with a low magnification and a binning factor of four. The exposure time was 23 ms with an effective pixel size of 106 μm. The total CT scan time process took approximately 15 minutes. The CT images were reconstructed using a Feldkamp conebeam back-projection algorithm provided by an Inveon Acquisition Workstation (IAW 2.1, Siemens). For the dynamic PET data acquisition, the emission data were normalized and corrected for radioactive time decay. The list-mode data were sorted into 41 frames (10 × 30 sec, 25 × 60 sec, 6 × 300 sec time frames). The resulting sinograms were reconstructed with FBP (filtered back-projection) and an ordered-subset expectation maximization (OSEM2D) algorithm and analysed using the Inveon Research Workplace software (IRW 4.1, Siemens) which allows fusion of CT and PET images and definition of region of interest (ROIs). For each PET image, 3D ROIs were drawn over the brain and other organs of interest guided by the CT using the IRW 4.1 software. Activity per voxel were converted to nci/cc using a conversion factor obtained by scanning a cylindrical phantom filled with a known activity of [^{18}F]fluoride to account for PET scanner efficiency. Activity concentrations were then expressed as percent of the decay-corrected injected activity per cm^3 of tissue that can be approximated as

percentage injected dose/g (%ID/g). Time activity curves (TACs) were drawn for each organ of interest including brain, heart, liver, kidney, guts and bladder.

3. Results and Discussion

*3.1. Synthesis of reference compound **4***

An overview of the synthetic route of reference compound **4** is presented in **Scheme 1**. Compound **1** was synthesized in two steps by iodination at the 3-position of 6-fluoroindole, followed by protection of the 1-*N*-position of the indole moiety with a Boc group. Initial attempts to make compound **3** by refluxing **1** with bis(pinacolato)diboron, KOAc, and Pd(dppf)Cl_2 in 1,4-dioxane at 80 ^{o}C for 5 h resulted in significant de-iodination. Compound **3** was subsequently synthesized using a method recently reported by Sigala *et al.*[20] Refluxing **1**: with pinacolborane, Et_3N and Pd(dppf)Cl_2 in toluene at 80°C for 3 h resulted in an 81% yield of **3** of with significantly less formation of de-iodinated compound.

Two different synthetic strategies were investigated to construct the C-C bond between the indole and pyridyl motifs to form compound **4**. The first approach which utilized Suzuki coupling of **3** with 3-bromopyridine on resulted in a 12% yield of compound **4**. Given the challenging purification of **3** and low yield of **4** *via* this synthetic route, an alternative synthesis for compound **4** was developed. Our alternative strategy involved the cross coupling of compound **1** with 3-(4,4,5,5,-tetramethyl-1,3,2-dioxaborolan-2-yl)pyridine (compound **2**). However the initial attempted synthesis of compound **2** by refluxing 3-bromopyridine with bis(pinacolato)diboron, KOAc and Pd(dppf)Cl_2 in 1,4-dioxane at 80°C for 20 h was unsuccessful. Increasing the amount of B_2pin_2, prolonging reaction time, elevating temperature, and changing solvent were investigated and these did not result in the synthesis of **2**. After further exploration of the literature, we utilized the method reported by Andersen *et al* in 2016[18] using *n*-BuLi and trimethoxyborane. By careful control of the

reaction temperature, **2** was obtained in 80% yield without the need for silica gel column purification. Reference compound **4** was synthesized *via* coupling **1** and **2** in DMSO at 90 ^{o}C for 3 h using K_2CO_3 as the base and Pd(dppf)Cl_2 as the catalyst. A yield of 30% was obtained using this method, which was almost 2.5 times greater than the previous synthetic routes attempted. It should be noted that the Boc group at indole 1-*N*-position was removed during the Suzuki coupling reaction.[28]

*3.2. Radiochemistry strategy and the synthesis of the radiolabeling precursor **8***

The 6-fluoro-indole position of our target compound **4** is not chemically reactive to traditional nucleophilic aromatic substitution and consequently attempts to form the corresponding 6-nitro or 6-trimethlyammonum derivative would result in no (or very low) radiochemical yields with fluorine-18. Recently Gouverneur *et al*[29] have demonstrated that aryl-boronate esters can be readily fluorinated in the presence of [Cu(py)$_4$](OTf). This led us to synthesize the labelling precursor *tert*-butyl 3-(pyridin-3-yl)-6-(4,4,5,5-tetramethyl-1,3,2-dioxaborolan-2-yl)-1H-indole-1-carboxylate **8** (**Scheme 2**). Since the reference compound **4** had already been synthesized, we initially decided to use **4** as a substrate to synthesize **7** *via* C-F bond cleavage. Methodology recently reported by Niwa *et al*[30] aroused our interest to transform **4** into **7** *via* Ni/Cu-catalyzed defluoroborylation reaction. Unfortunately, the desired product **7** was not obtained *via* this Ni/Cu-catalyzed defluoroborylation reaction. Switching to the 6-bromo derivative (**6**) proved a more successful approach since the bond energy of the C-Br bond is lower than that of the C-F bond. Compound **5** was synthesized in two steps *via* iodination of the 3-position of 6-bromoindole, followed by protection of the indole 1-*N*-position with a Boc group. Suzuki coupling of **5** with **2** in the presence of K_2CO_3 and Pd(dppf)Cl_2 gave compound **6** in 22% yield. Condensing **6** with bis(pinacolato)diboron in the presence of KOAc and Pd(dppf)Cl_2 at 90 ^{o}C for 24 h, followed by silica gel column afforded **7**. Finally, indole 1-*N*-position of compound **7** was protected with Boc group to afford compound **8** which was purified using HPLC. Since the Boc group can be thermally deprotected, in order to

avoid deprotection (and avoiding formation of **7**) the solvent was removed under vacuum without heating.

3.3. Radiochemistry

3.3.1 Radiochemistry development

Prior to radiolabelling compound **8**, pinacol phenylboronate was selected as a model compound to develop the experimental conditions required for the copper-mediated radiosynthesis (**Scheme 3**). Our initial manual radiosynthesis of [^{18}F]fluorobenzene indicated pinacol phenylboronate and $[Cu(py)_4](OTf)_2$ with molar ratio of 7 µmol: 9 µmol in 1 mL of DMA with air gave desired product with a decay corrected RCY of 22%. Further investigations demonstrated increasing amount of pinacol phenylboronate (50 µmol) and $[Cu(py)_4](OTf)_2$ (70 µmol) resulted in improving the RCY to 52%. However, since the current synthesis of precursor **8** has not currently been fully optimized, we have utilized lower quantities of the radiolabeling precursor **8** (7 µmol) and $[Cu(py)_4](OTf)_2$ (9 µmol) in our initial studies described in this paper since this should provide sufficient radiochemical yields for pre-clinical imaging assessment.

The initial radiolabeling of **8** (**Scheme 4**) at 120 ^{o}C revealed the presence of two radio-peaks (in addition to [^{18}F]fluoride) in the HPLC trace that eluted with retention times of 8.7 min and 18.7 minutes (**Figure 3a**) which have been attributed to [^{18}F]**4** and [^{18}F]**9** (the Boc-protected derivative of **4**) respectively. The predominant radiolabeled species at 120 ^{o}C is the Boc protected compound [^{18}F]**9** with a RCY of 18% (a small amount of [^{18}F]**4** with a RCY of 2% was also present). Given

the evidence of deprotection occurring during the labeling, we were concerned that the deprotection of the Boc-group from the precursor may also occur at 120°C and this may have had a negative impact on the radiochemical yield (since the indole *N*-H has the potential to hydrogen bond with the fluoride). In fact labelling the deprotected precursor (**7**) at 120°C resulted in a RCY of only 3%. Decreasing the labelling temperature of **8** to 100 °C eliminated deprotection, however resulted in a reduced radiochemical incorporation of fluorine-18 of only 8% at this temperature. Increasing the labelling temperature to 150 °C resulted in an increased level of deprotection of the Boc-group but resulted in a decreased overall incorporation of fluorine-18 to only 10% (**Figure 3b**), Zlatopolskiy et al. reported labelling in their studies was improved by using *tert*-butanol as a co-solvent (50:50 DMA: *tert*-butanol).[9] However, this did not significantly modify the radiochemical incorporation (RCY = 20%). Consequently the labelling temperature for the automation studies was fixed at 120 °C and the reaction were performed in 100% DMA.

3.3.2 Radiochemistry Automation

Researchers using copper-mediated nucleophilic [^{18}F]fluorination of aryl-boronate esters have indicated the importance of adding air during the radiolabeling step.[31] Whilst the introduction of air was relatively trivial for the manual labelling procedure (addition of air manually *via* a syringe) this initially presented a challenge for the automated platform (Synthra) that we use for our high activity radiosynthetic productions. This was primarily due to the fact that (i) the compressed air linked into the Synthra synthesis module is only linked into the cooling of the heater and (ii) helium gas is used to transfer reagents from the reagent vials (eg A1, A3, A4 of **Figure 4**) into the reaction vessel.

Consequently, after the drying step, the system is essentially under inert (helium atmospheric) conditions. In order to facilitate the introduction of air, we have modified the automation setup. **Figure 4** highlights that we have disconnected the line connection from **position 1** of the synthesis module (see highlighted section in yellow). Line 1 of the syringe system is now open to air and it is now possible to draw in air (from the hot cell environment) into to the syringe and then into the reaction vessel (after the addition of the radiolabeling precursors). However, since this syringe is

still normally wet after the clean-up of the synthesis module, we have now had to add an additional step to the protocol for the setup of the module. This now requires that, prior to synthesis, the syringe and the associated inlet ports (1 and 3) are dried thoroughly with helium. Additionally, since the air is delivered by the line from port 3 to the reaction vessel, the line connecting the syringe to the reaction vessel must also be thoroughly dried. The first part of the automation sequence (when air is required) now involves the syringe drawing up 1 mL of air from position 1. This means that by the time the sequence reaches the point when the labelling precursor and $[Cu(py)_4](OTf)_2$ are added from vial A3 to the reaction vessel, the syringe is primed to deliver the 1 mL of air into the reaction.

For the purposes of the testing this automation and to explore the benefits of the addition of air during the labelling step, we have tested this using the model compound pinacol phenylboronate (**Scheme 3**). This involved writing two sequences - one that involved the addition of the air and one that did not have air added. After the labelling, 1 mL of water was added to the reaction vessel (in order to re-dissolve any unreacted [^{18}F]fluoride) and the crude product was transferred into a vial and the reactions were analysed by HPLC. Our experiments have demonstrated that we can improve the RCY of the model compound from 22 ±2% (n = 2) to 29 ±3% (n=2) simply by the addition of air into the reaction vessel using the above modification of the synthesis module.

Following the positive impact of this modification of the Synthra automated module, we utilized this sequence for the automation of the automated radiolabeling of precursor **8**. During our manual labelling investigations, we observed that (i) the best radiochemical incorporation of fluorine-18 into our target compound was achieved at 120°C and (ii) the Boc-group is readily removed at 150 °C. Combining these two observations, for the automated radiosynthesis of [^{18}F]**4**, we have incorporated a labelling step of 120°C for 10 minutes (with the addition of 1 mL of air via the syringe) and included a thermal deprotection step after the labelling (5 minutes at 150°C). After labelling and deprotection, the reaction was allowed cool to 40°C before 1mL of water was added to dilute the crude reaction mixture. This diluted crude reaction mixture was the purified by HPLC.

Figure 5 shows an example of purification of the tracer using a semi-preparative HPLC column. After HPLC purification, the purified fraction was diluted into 60 mL of water and this was then subsequently trapped onto a C18 light Waters 130 mg solid phase extraction (SPE) cartridge. [^{18}F]**4** was eluted from the cartridge using 1 mL of ethanol into 9 mL of 0.9% saline.

However, the initial automated productions demonstrated evidence of radiolysis of the radiolabeled product even at relatively low radioactivite concentrations of 95 MBq/mL. To minimize this radiolysis, sodium ascorbate was added to the product saline solution as a stabilizer in subsequent radiosyntheses. Despite addition of 50 mg of sodium ascorbate in the saline, radiolysis was still observed in the final product. The HPLC trace of [^{18}F]**4** at t = 1 hour (after production) revealed that the radiochemical purity (RCP) of [^{18}F]**4** drops from 97% at t=0 to only 88% at t= 2 hour (for a production with a radioactive concentration of 159 MBq /mL). Addition of more sodium ascorbate (100 mg) in the saline and addition of sodium ascorbate in the mobile phase and in the collection vial used for dilution (both at 10 mg / mL) were then explored. These further modifications resulted in the formation of a stable product. Using this final method, [^{18}F]**4** was produced in isolated yields of 1.6 to 1.7 GBq (n = 3) with a radiochemical concentration of 160 to 170 MBq / mL. The non-corrected yield of these productions ranged from 5 to 6% and the RCP remained greater than 99% up to 4 h after end of synthesis (EOS) at room temperature (**Figure 6**). The molar activity of [^{18}F]**4** ranged from 214 to 261 GBq / µmol and the apparent molar activity (including other chemical impurities in the formulation ranged from 76 to 111 GBq / µmol). **Figure S1** confirms identity by HPLC and shows the co-injection of [^{18}F]F**4** with the ^{19}F reference standard. **Figure S2** displays the "zoomed in section" the UV trace of the HPLC from one of the stable final formulations [^{18}F]**4**. The area of the peak at approximately 6.3 minutes was used to calculate the molar activity and the total area of peaks at 5.9, 6.3 and 8.3 minutes were used to calculate the apparent molar activity of [^{18}F]**4**. **Figure S3** shows the calibration curve which was used to determine the quantity of chemical in the production of [^{18}F]**4**. For the purpose of the apparent molar activity, we have assumed that the

chemical species with peak retention times at 5.9 and 8.3 have similar absorption coefficients (and molecular weights) to **4**.

*3.3. Determination of lipophilicity (LogD) of **4***

The lipophilicity is a physical and chemical property of compound which provides an approximate reflection of its adsorption and distribution *in vivo*. A LogD value above 1 indicates that the compound probably can pass BBB just by diffusion. Secondly, non-specific binding is known to be higher with increasing lipophilicity among structurally relevant compound,[32] which revealed that the upper limit for LogD is estimated to 3.[33] The value of 1.8 found for **4** (n = 3) indicates that **4** possesses a suitable lipophilicity for the compound to cross the BBB.

3.4. Kinetic parameters for TDO

The kinetic parameters of compound **4** for TDO were determined using initial rate analysis. Initial rate data were fitted to Michaelis-Menten model. The inhibitory kinetics were evaluated by plotting 1/[S] against 1/[V], where [S] represents substrate concentration and [V] represents reaction rate. The Michaelis-Menten constant (Km) of TDO is 41.7 × μM and the binding constant is Ki=735 nM (see Supplementary for graph).

3.5. In vivo PET/CT imaging studies

In vivo dynamic PET/CT imaging studies were performed to evaluate the overall biodistribution of [^{18}F]**4** in normal healthy mice. Following intravenous injection of [^{18}F]**4** into C57BL/6 mice (n = 6), the tissue biodistribution was measured by PET/CT and summarized in **Figure 7**. [^{18}F]**4** localized rapidly to the heart and brain immediately after injection, reaching to the maximum occupancy in heart (10.9% ID/g) and brain (8.1% ID/g) at 1.75 min and 2.25 min, respectively. The radiolabeled compound was then steadily cleared from heart and brain, and taken up in liver, with 14% ID/g observed in the liver within the first 30 min. High levels of radioactivity were detected in kidney and bladder, suggesting excretion through kidney and bladder. A constant level of [^{18}F]**4** was found

in guts throughout the duration of the scan. Notably, tracer [^{18}F]**4** was not defluorinated *in vivo* on the time scale of the scan, as evidenced by the absence of [^{18}F]fluoride accumulation in bone (**Figure 8**). During the course of our investigations, the evaluation of several [^{18}F]-labelled IDO/TDO tracers have been reported. Henrottin *et al*[34] reported that 1-L-N-[^{18}F]FETrp showed higher affinity to hIDO compared to 1-D-*N*-[^{18}F]FETrp and 1-*L/D*-N-[^{18}F]FETrp. Small animal PET/CT imaging studies reported by Xin *et al*[7] revealed that tumour uptake of 1-L-N-[^{18}F]FETrp was 4.6 ± 04 %ID/g; in contrast 1-D-N-[^{18}F]FETrp uptake only 1.0 ± 0.2 %ID/g. In a recent report, Zlatopolskiy *et al*[9] radiosynthesized 4, 5, and 6-[^{18}F]FTrp from their corresponding pinacol boronate precursors. Whilst the 4, 5 and 6-[^{18}F]FTrp derivatives were stable *in vitro*, these radiolabelled tryptophan derivatives suffered from rapid defluorination *in vivo*. Tang *et al*[8] also highlighted failure of 5-L-[^{18}F]FTrp to cross the BBB in their study which they proposed was due to defluorination of this tracer *in vivo*. In contrast, [^{18}F]**4** showed high uptake in the liver and the brain and no evidence of defluorination *in vivo*, highlighting benefits of investigating this tracer in the future in tumor-burdened disease models.

4. Conclusion

We have radiosynthesized 6-[^{18}F]fluoro-3-(pyridine-3-yl)-1*H*-indole using a copper-mediated nucleophilic [^{18}F]fluorination of arenes method in a fully automated radiosynthesis module with non-corrected yield of 5 to 6% and a molar activity of 214 to 261 GBq / μmol. This study has demonstrated the need to include sodium ascorbate during the purification process and in the final formulation of [^{18}F]**4** to minimize radiolysis, which has resulted in the radiochemical purity of our final formulation of > 99% up to 4 hours post synthesis. Using dynamic PET/CT imaging studies we have demonstrated that 6-[^{18}F]fluoro-3-(pyridine-3-yl)-1*H*-indole has the ability to permeate the BBB and show no defluorination *in vivo* up to 1 hour following administration. Thus we propose

that [^{18}F]**4** warrants further exploration in oncology models as potential as a PET probe for imaging tryptophan metabolism *in vivo*.

5. Acknowledgements

The research was funded by the Australian Research Council Linkage grant #LP130100703. The authors acknowledge the facilities and scientific and technical assistance of the National Imaging Facility, a National Collaborative Research Infrastructure Strategy (NCRIS) capability, at the Centre for Advanced Imaging, University of Queensland. The authors would like to thank Dr Greg Pierens, Dr Brett Hamilton and Dr Lorine Wilkinson for additional support for the NMR, MS analysis and enzymatic essay, respectively. We would like to express gratitude to Dr Takashi Niwa (Chemical biology team, division of bio-function dynamics imaging, RIKEN centre for life science technologies) and Dr Masahiro Okada (Graduate school of pharmaceutical science, the university of Tokyo) for their warmly e-mail reply when acquiring experiment details of their publications.

Reference

1. Ott, M.; Litzenburger, U. M.; Rauschenbach, K. J.; Bunse, L.; Ochs, K.; Sahm, F.; Pusch, S.; Opitz, C. A.; Blaes, J.; von Deimling, A.; Wick, W.; Platten, M., Suppression of TDO-mediated tryptophan catabolism in glioblastoma cells by a steroid-responsive FKBP52-dependent pathway. *Glia* **2015,** *63* (1), 78-90.
2. Breda, C.; Sathyasaikumar, K. V.; Sograte Idrissi, S.; Notarangelo, F. M.; Estranero, J. G.; Moore, G. G. L.; Green, E. W.; Kyriacou, C. P.; Schwarcz, R.; Giorgini, F., Tryptophan-2,3-dioxygenase (TDO) inhibition ameliorates neurodegeneration by modulation of kynurenine pathway metabolites. *Proc. Natl. Acad. Sci. U. S. A.* **2016,** *113* (19), 5435-5440.
3. Siegel, R. L.; Miller, K. D.; Jemal, A., Cancer statistics, 2018. *CA-Cancer J. Clin.* **2018,** *68* (1), 7-30.
4. QUESNEL, B., Tumor dormancy and immunoescape *APMIS* **2008,** *116* (7-8), 685-694.
5. Huang, X.; Xiao, X.; Gillies, R. J.; Tian, H., Design and automated production of 11C-alpha-methyl-l-tryptophan (11C-AMT). *Nucl. Med. Biol.* **2016,** *43* (5), 303-308.
6. Xie, L.; Maeda, J.; Kumata, K.; Yui, J.; Zhang, Y.; Hatori, A.; Nengaki, N.; Wakizaka, H.; Fujinaga, M.; Yamasaki, T.; Shimoda, Y.; Higuchi, M.; Suhara, T.; Wang, F.; Zhang, M.-R., Development of 1-N-11C-Methyl-l- and -d-Tryptophan for pharmacokinetic imaging of the immune checkpoint inhibitor 1-Methyl-Tryptophan. *Sci Rep* **2015,** *5*, 16417.
7. Xin, Y.; Cai, H., Improved Radiosynthesis and Biological Evaluations of L- and D-1-[18F]Fluoroethyl-Tryptophan for PET Imaging of IDO-Mediated Kynurenine Pathway of Tryptophan Metabolism. *Mol. Imaging. Biol.* **2017,** *19* (4), 589-598.

8. Tang, T.; Gill, H. S.; Ogasawara, A.; Tinianow, J. N.; Vanderbilt, A. N.; Williams, S.-P.; Hatzivassiliou, G.; White, S.; Sandoval, W.; DeMent, K.; Wong, M.; Marik, J., Preparation and evaluation of L- and D-5-[18F]fluorotryptophan as PET imaging probes for indoleamine and tryptophan 2,3-dioxygenases. *Nucl. Med. Biol.* **2017,** *51*, 10-17.
9. Zlatopolskiy, B. D.; Zischler, J.; Schäfer, D.; Urusova, E. A.; Guliyev, M.; Bannykh, O.; Endepols, H.; Neumaier, B., Discovery of 7-[18F]Fluorotryptophan as a Novel Positron Emission Tomography (PET) Probe for the Visualization of Tryptophan Metabolism in Vivo. *J. Med. Chem.* **2018,** *61* (1), 189-206.
10. Juhász, C.; Chugani, D. C.; Muzik, O.; Wu, D.; Sloan, A. E.; Barger, G.; Watson, C.; Shah, A. K.; Sood, S.; Ergun, E. L.; Mangner, T. J.; Chakraborty, P. K.; Kupsky, W. J.; Chugani, H. T., In Vivo Uptake and Metabolism of α-[11C]Methyl-l-Tryptophan in Human Brain Tumors. *J. Cereb. Blood Flow Metab.* **2005,** *26* (3), 345-357.
11. Juhász, C.; Muzik, O.; Chugani, D. C.; Chugani, H. T.; Sood, S.; Chakraborty, P. K.; Barger, G. R.; Mittal, S., Differential kinetics of α-[11C]methyl-l-tryptophan on PET in low-grade brain tumors. *J. Neuro-Oncol.* **2011,** *102* (3), 409-415.
12. Mzengeza, S.; Venkatachalam, T. K.; Diksic, M., Asymmetric radiosynthesis of α-[11C]methyl-l-tryptophan for PET studies. *Nucl. Med. Biol.* **1995,** *22* (3), 303-307.
13. Chakraborty, P. K.; Mangner, T. J.; Chugani, D. C.; Muzik, O.; Chugani, H. T., A high-yield and simplified procedure for the synthesis of α-[11C]Methyl-l-tryptophan. *Nucl. Med. Biol.* **1996,** *23* (8), 1005-1008.
14. Rafice, Sara A.; Chauhan, N.; Efimov, I.; Basran, J.; Raven, Emma L., Oxidation of L-tryptophan in biology: a comparison between tryptophan 2,3-dioxygenase and indoleamine 2,3-dioxygenase. *Biochem. Soc. Trans.* **2009,** *37* (2), 408-412.
15. Hu, W.; Guo, Z.; Chu, F.; Bai, A.; Yi, X.; Cheng, G.; Li, J., Synthesis and biological evaluation of substituted 2-sulfonyl-phenyl-3-phenyl-indoles: a new series of selective COX-2 inhibitors. *Bioorg. Med. Chem.* **2003,** *11* (7), 1153-1160.
16. Crosignani, S.; Cauwenberghs, S.; Driessens, G.; Deroose, F. Novel 3-(indol-3-yl)-pyridine derivatives, pharmaceutical compositions and methods for use. **WO2015121812A1**, 2015.
17. Witulski, B.; Buschmann, N.; Bergsträßer, U., Hydroboration and Suzuki–Miyaura Coupling Reactions with the Electronically Modulated Variant of an Ynamine: The Synthesis of (E)-β-Arylenamides. *Tetrahedron* **2000,** *56* (43), 8473-8480.
18. Andersen, T. L.; Frederiksen, M. W.; Domino, K.; Skrydstrup, T., Direct Access to α,α-Difluoroacylated Arenes by Palladium-Catalyzed Carbonylation of (Hetero)Aryl Boronic Acid Derivatives. *Angew. Chem.-Int. Edit.* **2016,** *55* (35), 10396-10400.
19. Jia, Y.; Bois-Choussy, M.; Zhu, J., Synthesis of DEFG Ring of Complestatin and Chloropeptin I: Highly Atropdiastereoselective Macrocyclization by Intramolecular Suzuki-Miyaura Reaction. *Org. Lett.* **2007,** *9* (12), 2401-2404.
20. Sigala, I.; Ganidis, G.; Thysiadis, S.; Zografos, A. L.; Giannakouros, T.; Sarli, V.; Nikolakaki, E., Lynamicin D an antimicrobial natural product affects splicing by inducing the expression of SR protein kinase 1. *Bioorg. Med. Chem.* **2017,** *25* (5), 1622-1629.
21. Song, J.; Wang, Q.; Fu, H.; Fu, S.; Li, S.; Shi, F.; Wu, C., Copper-Catalyzed N-Alkynylation of N-tert-Butyloxycarbonyl (Boc)-Protected Indoles. *Asian J. Org. Chem.* **2013,** *2* (10), 877-881.
22. Okada, M.; Sugita, T.; Wong, C. P.; Wakimoto, T.; Abe, I., Identification of Pyridinium with Three Indole Moieties as an Antimicrobial Agent. *J. Nat. Prod.* **2017,** *80* (4), 1205-1209.
23. Taylor, N. J.; Emer, E.; Preshlock, S.; Schedler, M.; Tredwell, M.; Verhoog, S.; Mercier, J.; Genicot, C.; Gouverneur, V., Derisking the Cu-Mediated 18F-Fluorination of Heterocyclic Positron Emission Tomography Radioligands. *J. Am. Chem. Soc.* **2017,** *139* (24), 8267-8276.
24. Tasch, B. O. A.; Antovic, D.; Merkul, E.; Müller, T. J. J., One-Pot Synthesis of Camalexins and 3,3'-Biindoles by the Masuda Borylation–Suzuki Arylation (MBSA) Sequence. *Eur. J. Org. Chem.* **2013,** *2013* (21), 4564-4569.
25. Stimson, D.; Qiao, Z.; C Reutens, D.; Venkatachalam, T.; Bhalla, R., Investigation on the impact of three different QMA cartridges on the radiosynthetic yields of [18F]fluoromethyl tosylate. *Journal of Labelled Compounds and Radiopharmaceuticals* **2019,** *62*.
26. Giglio, B. C.; Fei, H.; Wang, M.; Wang, H.; He, L.; Feng, H.; Wu, Z.; Lu, H.; Li, Z., Synthesis of 5-[(18)F]Fluoro-α-methyl Tryptophan: New Trp Based PET Agents. *Theranostics* **2017,** *7* (6), 1524-1530.

27. Huang, Q.; Zheng, M.; Yang, S.; Kuang, C.; Yu, C.; Yang, Q., Structure–activity relationship and enzyme kinetic studies on 4-aryl-1H-1,2,3-triazoles as indoleamine 2,3-dioxygenase (IDO) inhibitors. *Eur. J. Med. Chem.* **2011,** *46* (11), 5680-5687.
28. Gan, T.; Liu, R.; Yu, P.; Zhao, S.; Cook, J. M., Enantiospecific Synthesis of Optically Active 6-Methoxytryptophan Derivatives and Total Synthesis of Tryprostatin A1. *J. Org. Chem.* **1997,** *62* (26), 9298-9304.
29. Tredwell, M.; Preshlock, S. M.; Taylor, N. J.; Gruber, S.; Huiban, M.; Passchier, J.; Mercier, J.; Génicot, C.; Gouverneur, V., A General Copper-Mediated Nucleophilic 18F Fluorination of Arenes. *Angewandte Chemie* **2014,** *126* (30), 7885-7889.
30. Niwa, T.; Ochiai, H.; Watanabe, Y.; Hosoya, T., Ni/Cu-Catalyzed Defluoroborylation of Fluoroarenes for Diverse C–F Bond Functionalizations. *J. Am. Chem. Soc.* **2015,** *137* (45), 14313-14318.
31. Taylor, N. J.; Emer, E.; Preshlock, S.; Schedler, M.; Tredwell, M.; Verhoog, S.; Mercier, J.; Genicot, C.; Gouverneur, V., Derisking the Cu-Mediated 18F-Fluorination of Heterocyclic Positron Emission Tomography Radioligands. *Journal of the American Chemical Society* **2017,** *139* (24), 8267-8276.
32. Pike, V. W., PET radiotracers: crossing the blood-brain barrier and surviving metabolism. *Trends Pharmacol Sci.* **2009,** *30* (8), 431-440.
33. Dischino, D. D.; Welch, M. J.; Kilbourn, M. R.; Raichle, M. E., Relationship Between Lipophilicity and Brain Extraction of C-11-Labeled Radiopharmaceuticals. *J. Nucl. Med.* **1983,** *24* (11), 1030-1038.
34. Henrottin, J.; Lemaire, C.; Egrise, D.; Zervosen, A.; Van den Eynde, B.; Plenevaux, A.; Franci, X.; Goldman, S.; Luxen, A., Fully automated radiosynthesis of N1-[18F]fluoroethyl-tryptophan and study of its biological activity as a new potential substrate for indoleamine 2,3-dioxygenase PET imaging. *Nucl. Med. Biol.* **2016,** *43* (6), 379-389.

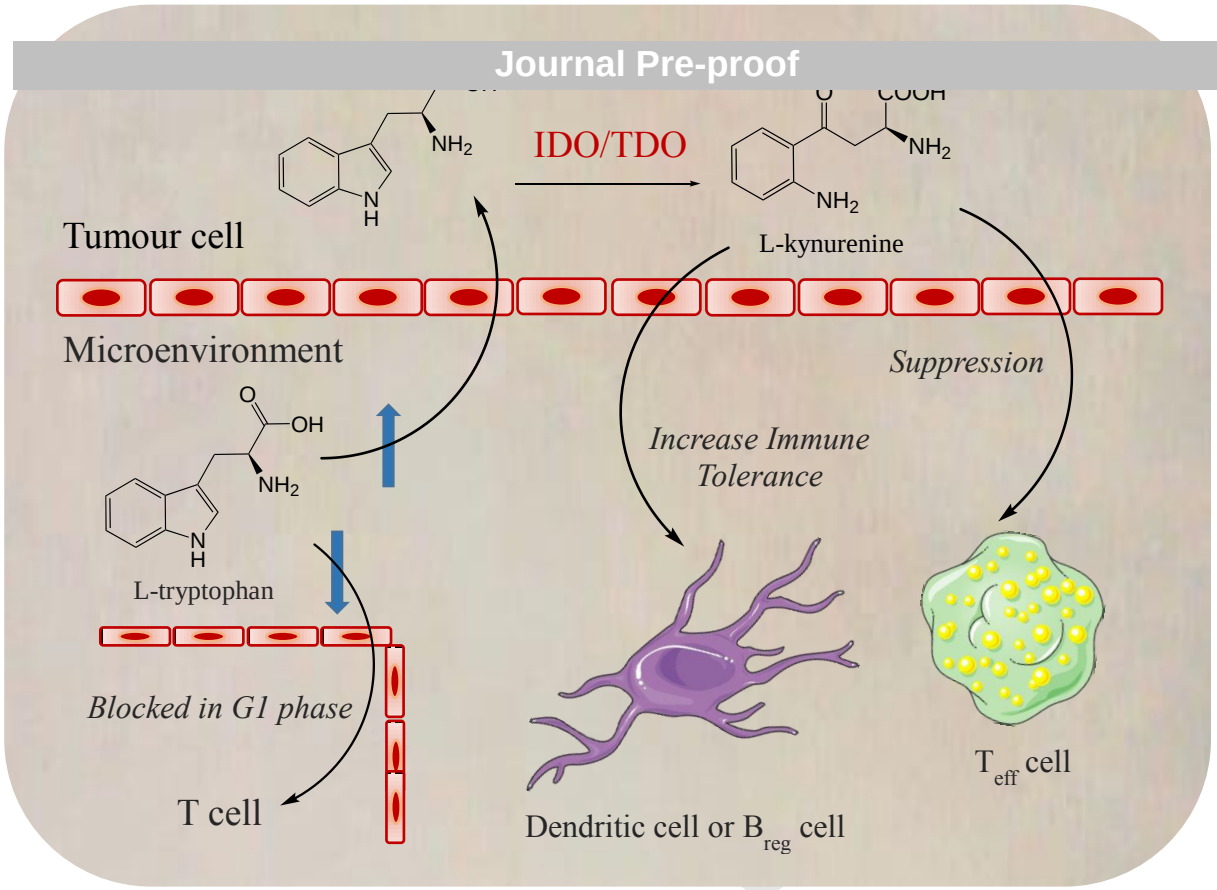

Figure 1.

Zheng Qiao *et al*

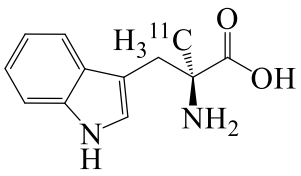

[^{11}C]AMT

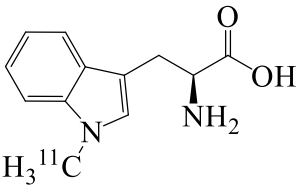

L-[^{11}C]1MTrp

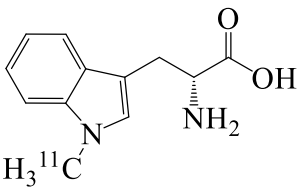

D-[^{11}C]1MTrp

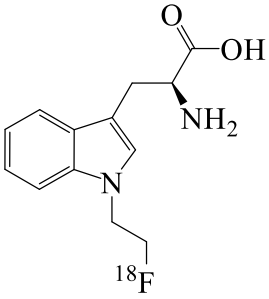

1-*L*-*N*-[^{18}F]FETrp

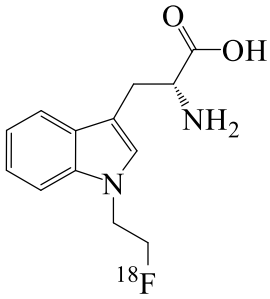

1-*D*-*N*-[^{18}F]FETrp

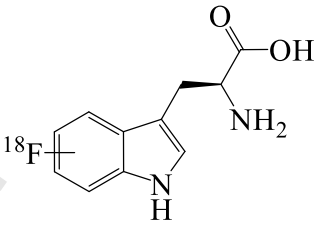

4, 5, 6-[^{18}F]FTrp

Figure 2.

Zheng Qiao *et al*

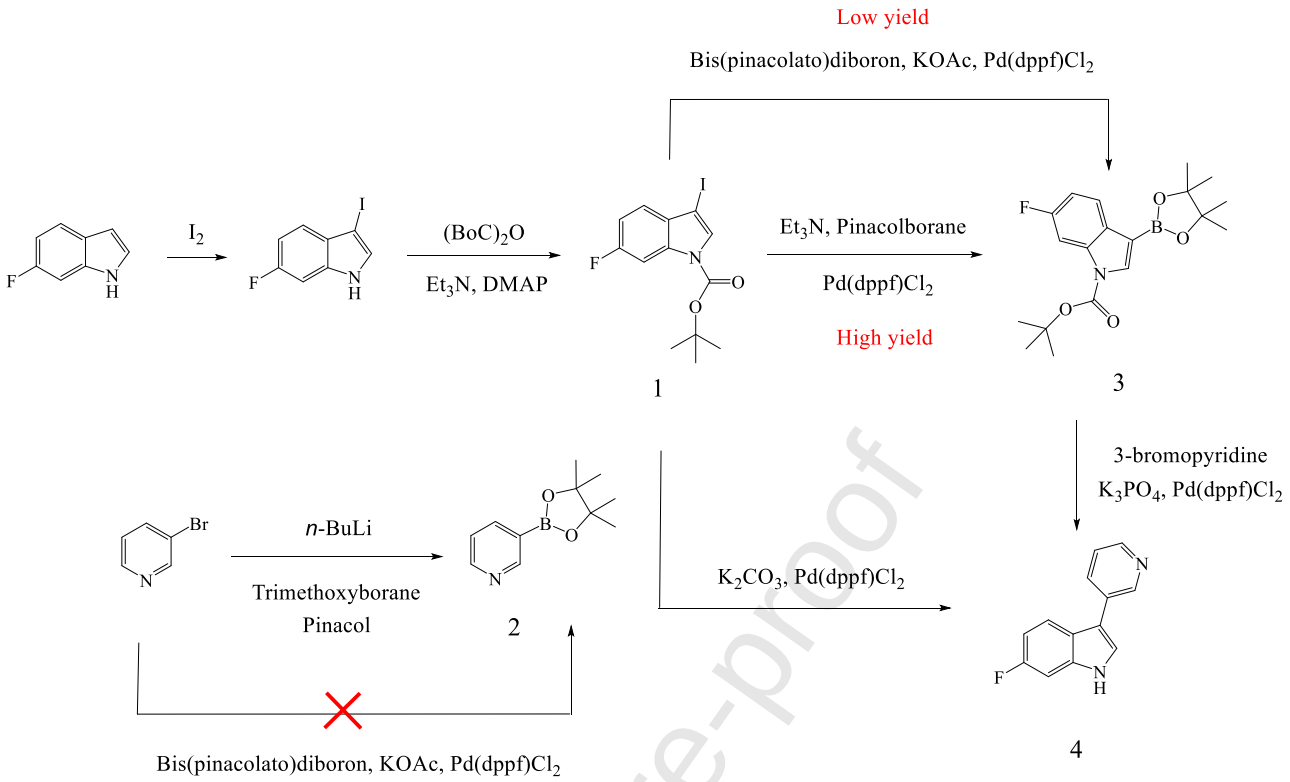

Scheme 1.

Zheng Qiao *et al*

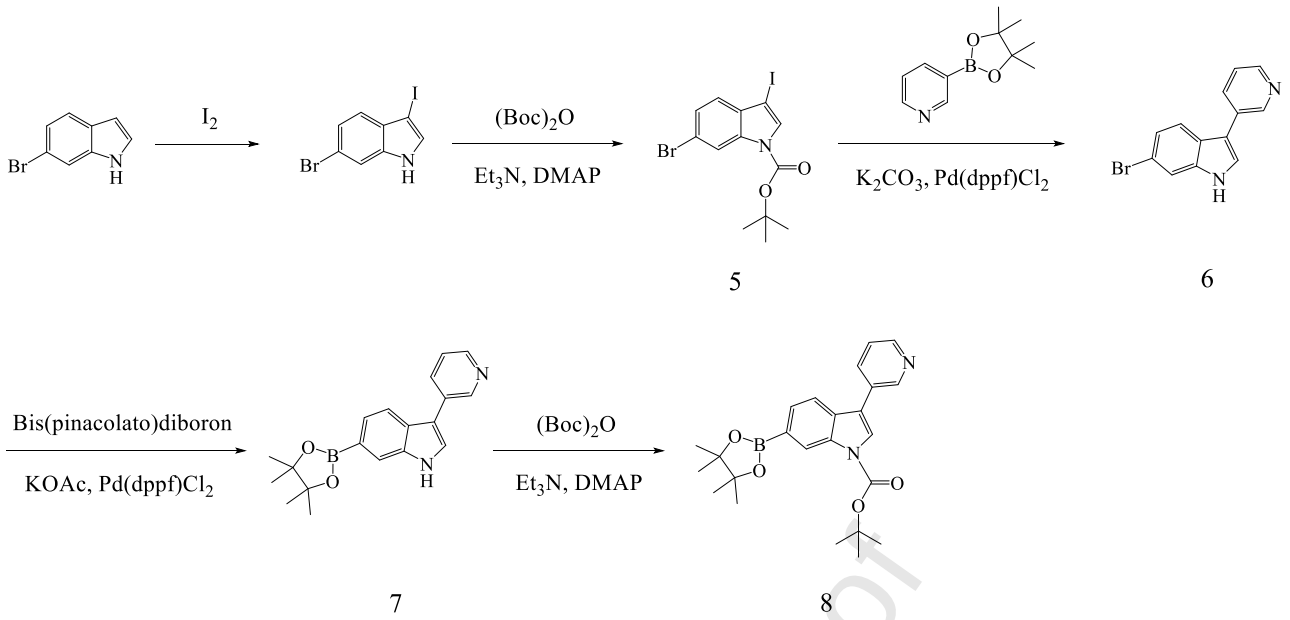

5 6 7 8

Scheme 2.

Zheng Qiao *et al*

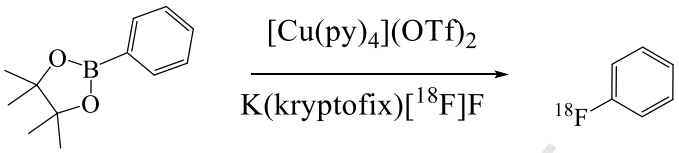

Scheme 3.

Zheng Qiao *et al*

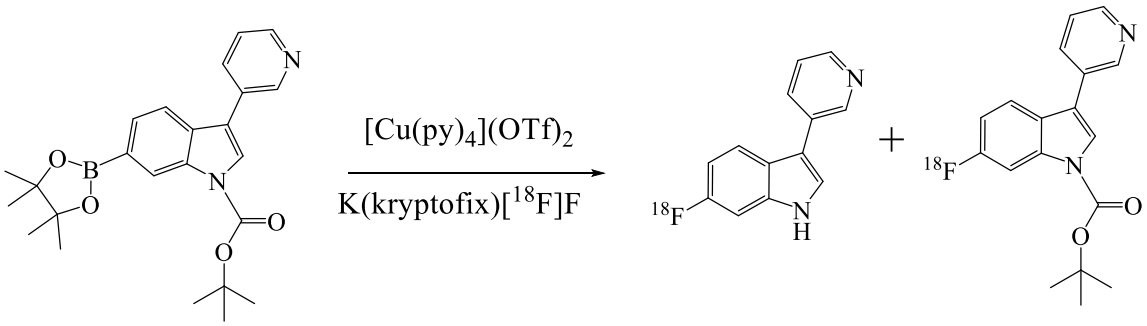

8 [^{18}F]**4** [^{18}F]**9**

Scheme 4.

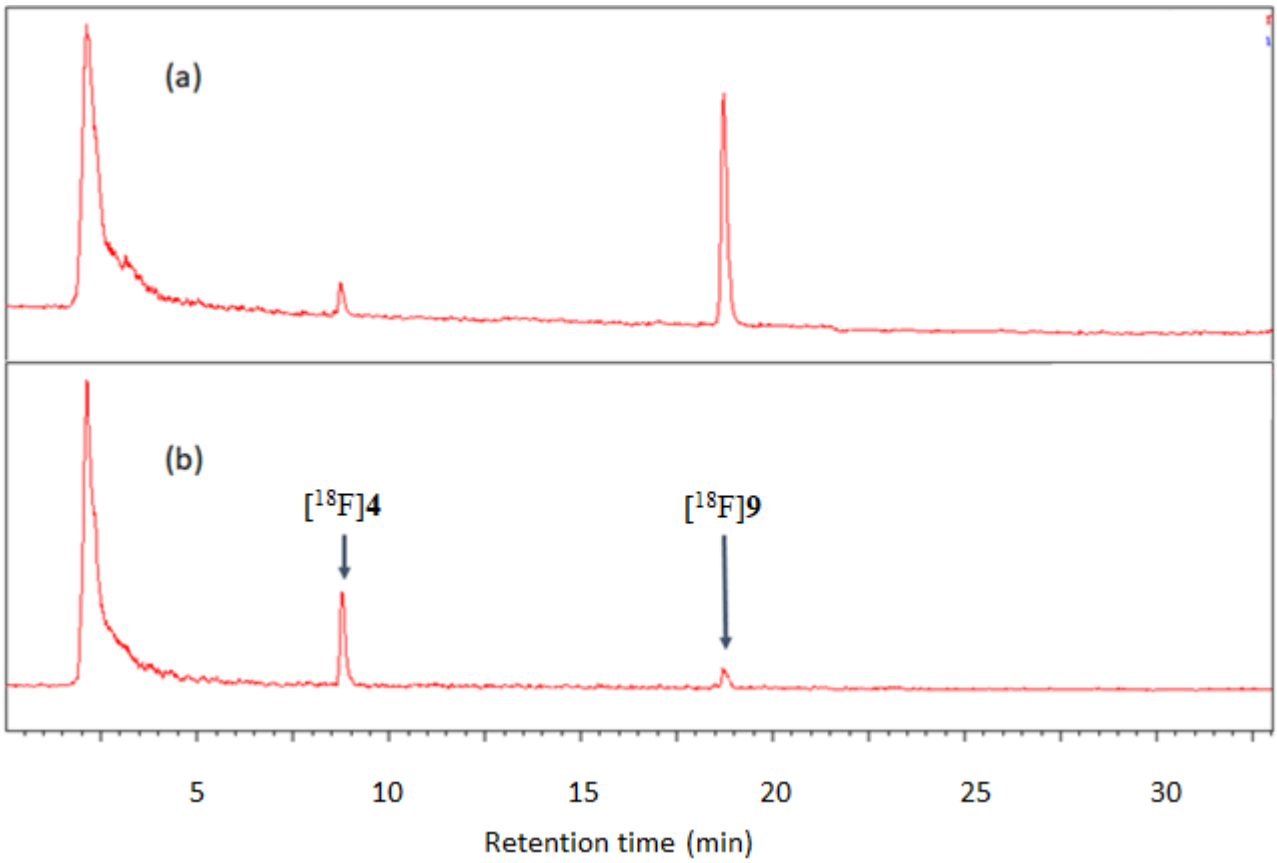

Figure 3.

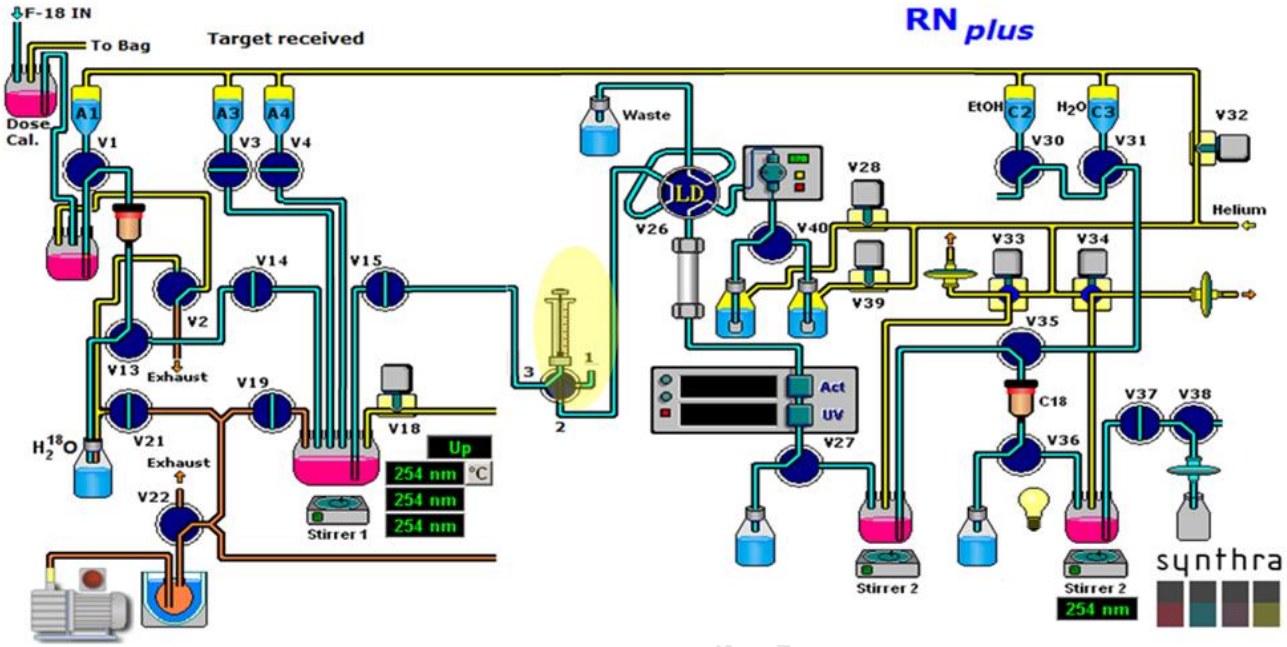

Figure 4.

Zheng Qiao *et al*

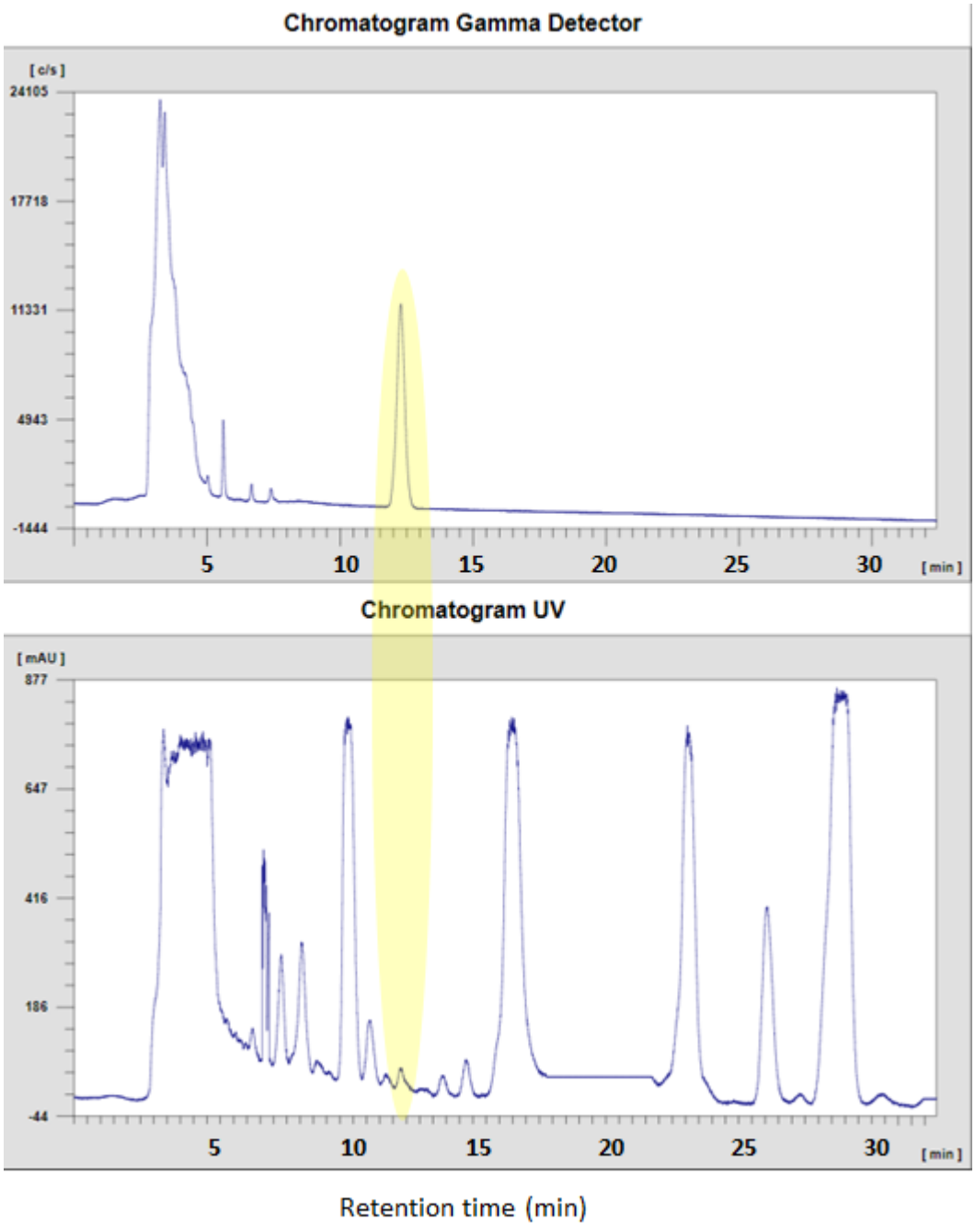

Figure 5.

Zheng Qiao *et al*

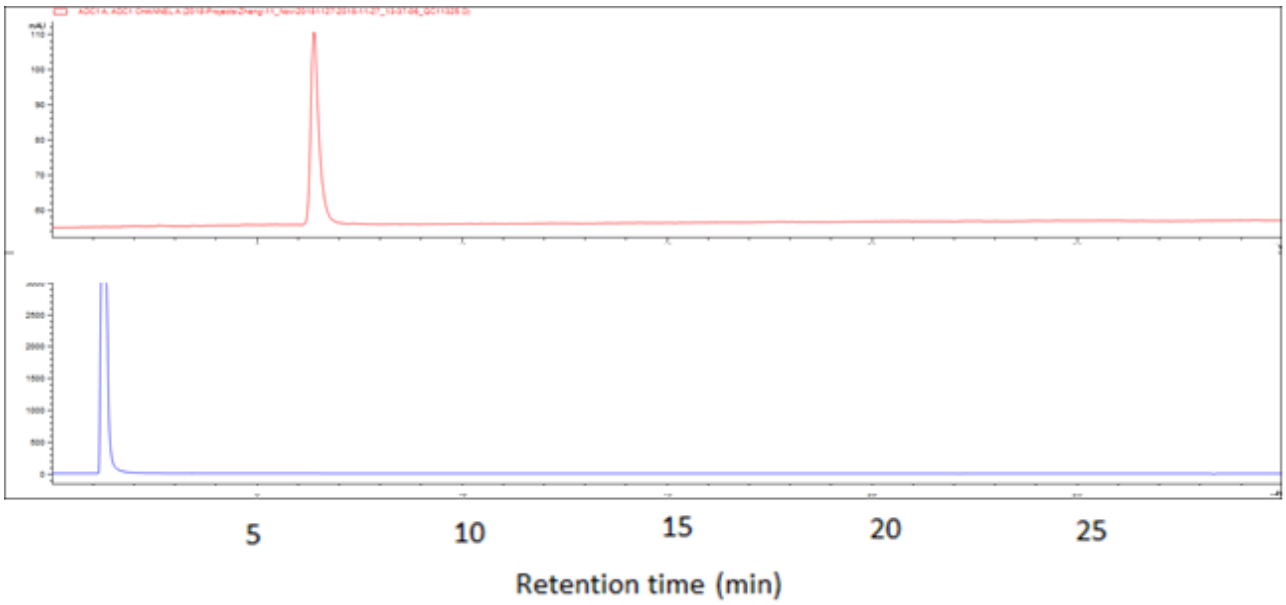

Figure 6.

Zheng Qiao *et al*

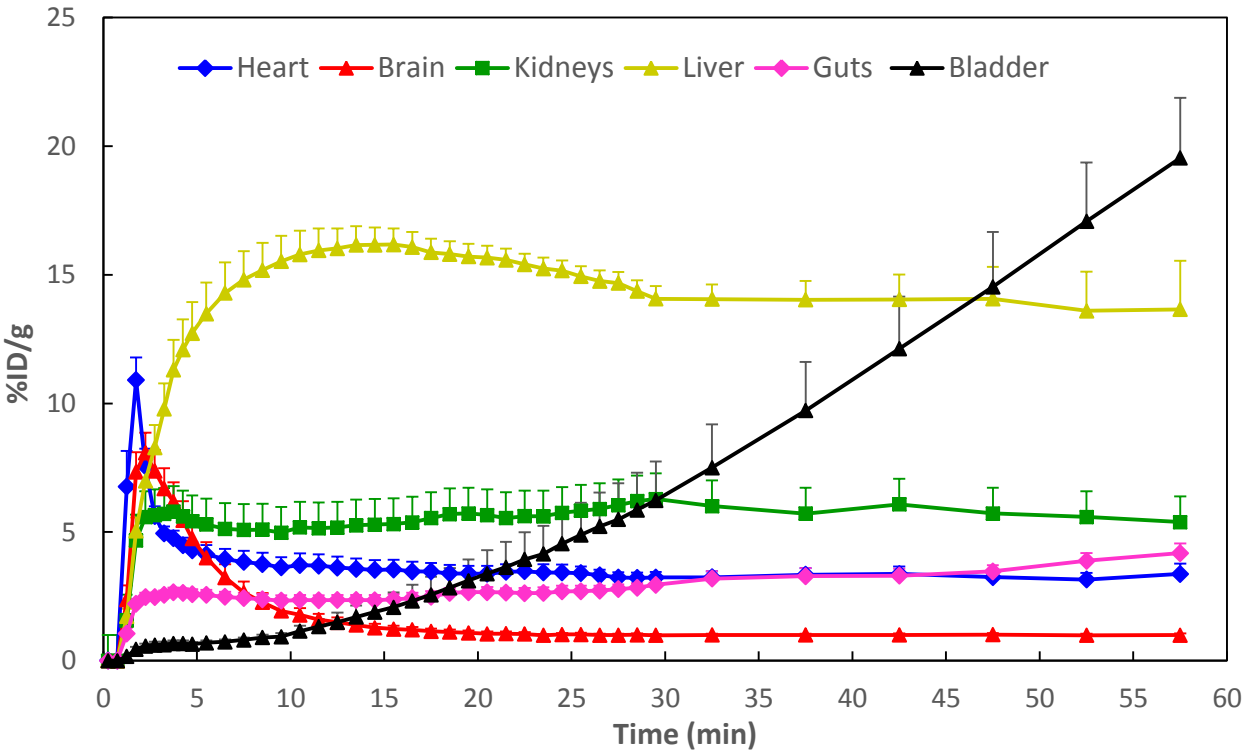

Figure 7.

Zheng Qiao *et al*

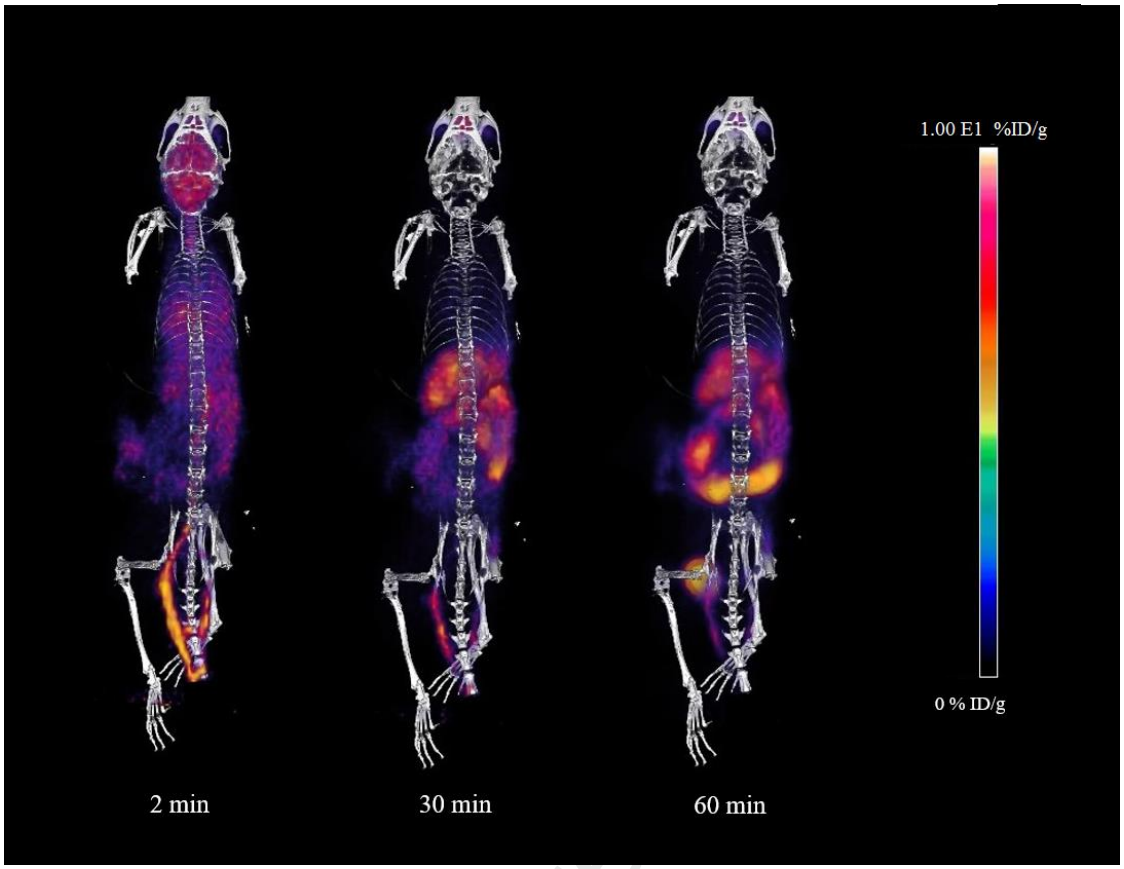

Figure 8.

Zheng Qiao *et al*

Figure Captions:

Figure 1. The kynurenine pathway of tumour immunoescape.

Figure 2. Representative PET tracers of kynurenine pathway.

Scheme 1. The overview of synthetic route of reference compound **4.**

Scheme 2: The overview of synthetic route of radiolabelling precursor **8.**

Scheme 3: Radiosynthetic route of [^{18}F]fluorobenzene *via* copper-mediated nucleophilic [^{18}F]fluorination method.

Scheme 4: Radiolabelling of precursor **8.**

Figure 3. HPLC of radiolabelling precursor **8** at (a) 120 °C and (b) 150 °C using HPLC Method 1

Figure 4. Scheme illustrating modified layout of the Synthra automated synthesis module.

Figure 5 HPLC purification of [^{18}F]**4** performed on automated Synthra module using an Eclipse XDB-C18 Semi-Prep 5µm,. Mobile phase: 40% MeCN / 60% 0.1 M NH_4OAc with a constant flow rate of 4 mL/min. Highlighted section shows the HPLC purified fraction.

Figure 6. Radio-HPLC of [^{18}F]**4** in the formulation after adding 100 mg of sodium ascorbate in the final formulation vial (4 h after EOS at room temperature) using HPLC Method 2. The large UV peak at approximately 1.5 minutes is due to the sodium ascorbate in the final formulation.

Figure 7. Biodistribution of tracer [^{18}F]**4** following i.v. injection in control mice (n=6) measured using PET-CT over 60 min. Data presented as mean ± SEM (standard error of the mean)

Figure 8. Dynamic PET/CT images of normal C57BL/6 mice at 2, 30 and 60 min following intravenous injection of [^{18}F]**4**.